EUROPEAN ORGANIZATION FOR NUCLEAR RESEARCH

LEPEWWG/TGC/2000-02
ALEPH 2000-081 PHYSIC 2000-028
DELPHI 2000-155 PHYS 871
L3 Note 2604
OPAL TN-663
September 21st, 2000

Combined Preliminary Results on Electroweak Gauge Boson Couplings Measured by the LEP Experiments

The LEP Collaborations ALEPH, DELPHI, L3, OPAL, and the LEP TGC Working Group*

Prepared from contributions of the LEP experiments to the summer conferences 2000.

Abstract

This note presents a combination of published and preliminary results on electroweak gauge boson couplings measured by the four LEP experiments, including both triple (TGC) and quartic (QGC) gauge boson couplings. Besides the charged TGCs g_1^Z, κ_γ and λ_γ, and the neutral TGCs h_i^V and f_i^V, the charged TGC g_5^Z and the QGCs a_0/Λ^2, a_c/Λ^2 and a_n/Λ^2 are also combined for the first time.

*Contact: Martin W. Grünewald, e-mail: `Martin.Grunewald@cern.ch`
The collaborations each take responsibility for the preliminary data of their own experiment.
WWW access at `http://www.cern.ch/LEPEWWG/tgc/`

1 Introduction

During the second phase of its operation, which started in 1996, the e^+e^- collider LEP at CERN steadily increased its centre-of-mass energy, from 161 GeV to 209 GeV reached this year. Until the end of 1999, a total luminosity of approximately 475 pb^{-1} per experiment was recorded at LEP2. This year's data taking is still in progress; an additional luminosity of about 90 pb^{-1} per experiment has been recorded until July.

The W-pair production process, $e^+e^- \to W^+W^-$, involves the triple gauge boson vertices between the W^+W^- and the Z or the photon. Until the end of 1999, more than 7000 W-pair events are collected by each experiment. Single W ($e\nu W$) and single photon ($\nu\bar{\nu}\gamma$) production at LEP are sensitive to the $WW\gamma$ vertex. The measurement of these charged triple gauge boson couplings and the search for possible anomalous contributions due to the effects of new physics beyond the Standard Model is one of the principal physics goals at LEP2 [1].

At centre-of-mass energies exceeding twice the Z boson mass, pair production of Z bosons is kinematically allowed. Here, one searches for the possible existence of triple vertices involving only neutral electroweak gauge bosons. Such vertices could also contribute to $Z\gamma$ production. In contrast to triple gauge boson vertices with two charged gauge bosons, purely neutral gauge boson vertices do not occur in the Standard Model of electroweak interactions.

Within the Standard Model, quartic electroweak gauge boson vertices with at least two charged gauge bosons exist. In e^+e^- collisions at LEP2 centre-of-mass energies, the $WWZ\gamma$ and $WW\gamma\gamma$ vertices contribute to $WW\gamma$ and $\nu\bar{\nu}\gamma\gamma$ production in s-channel and t-channel, respectively. The effect of the Standard Model quartic electroweak vertices is below the sensitivity of LEP2. Thus, anomalous quartic vertices are searched for in the production of $WW\gamma$ and $\nu\bar{\nu}\gamma\gamma$ but also $Z\gamma\gamma$ final states.

In this note we present the combination of results on electroweak gauge boson couplings based on the data collected by the four LEP experiments at LEP2. Charged TGCs [2–5], neutral TGCs [6–11] as well as QGCs [12–14] are combined.

2 Electroweak Gauge Boson Couplings

2.1 Charged Triple Gauge Boson Couplings

The parametrisation of the charged triple gauge boson vertices is described in References [1,15–20]. The most general Lorentz invariant Lagrangian which describes the charged triple gauge boson interaction contains fourteen independent complex couplings, seven describing the $WW\gamma$ vertex and seven describing the WWZ vertex. Assuming electromagnetic gauge invariance as well as CP conservation, the number of independent TGCs reduces to six. One common set is $\{g_1^Z, \kappa_\gamma, \kappa_Z, \lambda_\gamma, \lambda_Z, g_5^Z\}$ where $g_1^Z = \kappa_\gamma = \kappa_Z = 1$ and $\lambda_\gamma = \lambda_Z = g_5^Z = 0$ in the Standard Model. Except g_5^Z, all these couplings also conserve C and P separately.

The parameters proposed in [1] and used here are:

$$\Delta g_1^{\mathrm{Z}} \equiv g_1^{\mathrm{Z}} - 1\,, \tag{1}$$
$$\Delta\kappa_\gamma \equiv \kappa_\gamma - 1\,, \tag{2}$$
$$\lambda_\gamma \quad , \tag{3}$$
$$g_5^{\mathrm{Z}} \quad , \tag{4}$$

with the gauge constraints:

$$\Delta\kappa_{\mathrm{Z}} \equiv \kappa_{\mathrm{Z}} - 1 = \Delta g_1^{\mathrm{Z}} - \Delta\kappa_\gamma \tan^2\theta_W \tag{5}$$
$$\lambda_{\mathrm{Z}} = \lambda_\gamma\,, \tag{6}$$

where Δ indicates the deviation of the respective coupling from its Standard Model value of unity, and θ_W is the weak mixing angle. The couplings are considered as real, with the imaginary parts fixed to zero.

2.2 Neutral Triple Gauge Boson Couplings

There are two possible anomalous triple vertices in the neutral sector. Each is parametrised by the most general Lorentz and $U(1)_{em}$ invariant Lagrangian plus Bose symmetry, as described in References [16, 21].

The first vertex refers to anomalous Z$\gamma\gamma$ and ZZγ couplings which are accessible at LEP in the process $\mathrm{e^+e^-} \to \mathrm{Z}\gamma$. The parametrisation contains eight couplings: h_i^V with $i = 1, ..., 4$ and $V = \gamma$,Z. The superscript γ refers to Z$\gamma\gamma$ couplings and superscript Z refers to ZZγ couplings. The photon and the Z boson in the final state are considered as on-shell particles, while the third boson at the triple vertex is off shell. The couplings h_1^V and h_2^V are CP-odd while h_3^V and h_4^V are CP-even.

The second vertex refers to anomalous ZZγ and ZZZ couplings which are accessible at LEP in the process $\mathrm{e^+e^-} \to \mathrm{ZZ}$. This anomalous vertex is parametrised in terms of four couplings: f_i^V with $i = 4, 5$ and $V = \gamma$,Z. The superscript γ refers to ZZγ couplings and the superscript Z refers to ZZZ couplings. Both Z bosons in the final state are assumed to be on-shell, while the third boson at the triple vertex is off-shell. The couplings f_4^V are CP-odd whereas f_5^V are CP-even.

Note that the h_i^V and f_i^V couplings are independent of each other. They are considered as real, with the imaginary parts fixed to zero. They vanish in the Standard Model at tree level.

2.3 Quartic Gauge Boson Couplings

Anomalous contributions to electroweak quartic vertices are considered in the framework of References [22–24]. Three lowest-dimensional operators leading to quartic vertices not causing anomalous TGCs are considered. The corresponding couplings are a_0/Λ^2, a_c/Λ^2 and a_n/Λ^2, where Λ represents the energy scale of new physics. The couplings a_0/Λ^2 and a_c/Λ^2 parametrise

variations in the WW$\gamma\gamma$ and ZZ$\gamma\gamma$ vertices, while a_n/Λ^2 affects purely the WWZγ vertex. The couplings a_0/Λ^2 and a_c/Λ^2 conserve C and P, while the coupling a_n/Λ^2 is CP violating. The production of WWγ depends on all three couplings. The production of $\nu\bar{\nu}\gamma\gamma$ and Z$\gamma\gamma$ depends only on a_0/Λ^2 and a_c/Λ^2, the former through the WW$\gamma\gamma$ vertex, the latter through the ZZ$\gamma\gamma$ vertex. The couplings are considered as real, with the imaginary parts fixed to zero. They vanish in the Standard Model at tree level.

A more detailed description of QGCs has recently appeared [25], in which it is suggested that the coupling a_0/Λ^2 and a_c/Λ^2 describing the anomalous WW$\gamma\gamma$ vertex should not be assumed to be the same couplings as those describing the anomalous ZZ$\gamma\gamma$ vertex. The experimental results on these vertices are therefore also given separately.

3 Measurements

The results presented comprise measurements of all electroweak gauge boson couplings discussed above. In most cases, the results are based on the data collected at LEP2 until the end of 1999 at centre-of-mass energies up to 202 GeV. The experiments already combine different processes and final states for each coupling. In each case, the individual references should be consulted for the details on the data samples used.

For charged TGCs, the experimental analyses study different channels, typically the semileptonic, fully hadronic and fully leptonic W-pair decays [2–5]. Anomalous TGCs affect both the total production cross-section and the shape of the differential cross-section as a function of the polar W^- production angle. The relative contributions of each helicity state of the W bosons are also changed, which in turn affects the distributions of their decay products. The analyses presented by each experiment make use of different combinations of each of these quantities. In general, however, all analyses use at least the expected variations of the total production cross-section and the W^- production angle. Results from eνW and $\nu\bar{\nu}\gamma$ production are included by some experiments. Single W production is particularly sensitive to κ_γ, thus providing information complementary to that from W-pair production.

For neutral TGCs, the analyses use mainly measurements of the total cross sections of Zγ and ZZ production, though the use of differential distributions increases the sensitivity. The individual references should be consulted concerning the details of the analyses for the h_i^V couplings [6–8] and the f_i^V couplings [9–11].[1]

For QGCs, the experiments investigate WWγ, $\nu\bar{\nu}\gamma\gamma$ and Z$\gamma\gamma$ production. Besides the total cross section, the sensitive variables analysed are photon energies (WWγ and Z$\gamma\gamma$) and recoil masses ($\nu\bar{\nu}\gamma\gamma$). Again, the individual references should be consulted for the details in the determination of the QGCs a_0/Λ^2, a_c/Λ^2 and a_n/Λ^2 [12–14].

[1]For quoting results on the f_i^V couplings, DELPHI [9] uses a convention for the sign of f_i^V opposite to that used by L3 [10] and OPAL [11]. For DELPHI and combined LEP results presented in this note, the DELPHI f_i^V measurements have been modified to conform to the same sign convention as used by L3 and OPAL.

4 Combination Procedure

The combination procedure is modified compared to previous LEP combinations of electroweak gauge boson couplings [26, 27] in order to treat systematic uncertainties correlated between the experiments.

Each experiment provides the negative log likelihood, $\log \mathcal{L}$, as a function of the coupling parameters (one, two, or three) to be combined. The single parameter analyses are performed fixing the values of all other parameters to their Standard Model value. The two- and three-parameter analyses are performed setting the remaining parameters to their Standard Model value. For the charged TGCs, the gauge constraints listed in Section 2.1 are always enforced.

The $\log \mathcal{L}$ functions from each experiment include statistical as well as all systematic uncertainties considered as uncorrelated between experiments. For both single- and multi-parameter combinations, the individual $\log \mathcal{L}$ functions are added. It is necessary to use the $\log \mathcal{L}$ functions directly for the combination as in some cases they are not parabolic, so that it is not possible to combine the results correctly by simply taking weighted averages of the measurements.

The main contributions to the systematic uncertainties uncorrelated between experiments arise from detector effects, background in the selected signal samples, limited Monte Carlo statistics and fitting method. Their importance varies for each experiment and the individual references should be consulted for details.

The systematic uncertainties arising from the following sources are treated as correlated between the experiments: the uncertainty on the theoretical cross section prediction ($\mathrm{W^+W^-}$, $\mathrm{e\nu W}$ and $\mathrm{Z\gamma}$ production), fragmentation effects ($\mathrm{W^+W^-}$ production), and Bose-Einstein correlations and colour-reconnection effects (fully hadronic W-pair decays). While the correlated systematic uncertainties are small in $\mathrm{Z\gamma}$ production, they are sizeable for charged TGCs, see Appendix A. In particular, the uncertainty on the theoretical cross section prediction for the $\mathrm{e\nu W}$ process causes a large reduction in the sensitivity of this process to charged TGCs. For ZZ production, the uncertainty on the theoretical cross section prediction is small compared to the statistical accuracy and neglected. For other sources of correlated systematic uncertainties, such as those arising from the LEP beam energy or the W mass, the effect of their correlation on the combination result is negligible.

The correlated systematic uncertainties are applied by scaling the likelihood functions by the squared ratio of the statistical and uncorrelated systematic uncertainty over the total uncertainty including all correlated uncertainties. This procedure to treat correlations is an approximation in the case where the log-likelihood function is not parabolic.

The one standard deviation uncertainties (68% confidence level) are obtained by taking the coupling values where $\Delta \log \mathcal{L} = +0.5$ above the minimum. The 95% confidence level (C.L.) limits are given by the coupling values where $\Delta \log \mathcal{L} = +1.92$ above the minimum. These cut-off values are used for obtaining the results of both single- and multi-parameter analyses reported here. Note that in the case of the neutral TGCs and the QGCs, double minima structures appear in the negative log-likelihood curves. For multi-parameter analyses, the 68% C.L. contour curves for any pair of couplings are obtained by requiring $\Delta \log \mathcal{L} = +1.15$, while for the 95% C.L. contour curves $\Delta \log \mathcal{L} = +3.0$ is required.

5 Results

We present below results from the four LEP experiments on the various electroweak gauge boson couplings, and their combination. Also the results quoted individually for each experiment are calculated using the method described in Section 4. Thus they may differ slightly from those reported in the individual references.

5.1 Charged Triple Gauge Boson Couplings

Single-Parameter Analyses

The results from each experiment are shown in Table 1, where the uncertainties include both statistical and systematic effects. The individual $\log \mathcal{L}$ curves and their sum are shown in Figure 1. The results of the combination are given in Table 2.

Two-Parameter Analyses

The results from each experiment are shown in Table 3, where the uncertainties include both statistical and systematic effects. The 68% C.L. and 95% C.L. contours curves resulting from the combinations of the two-dimensional likelihood curves are shown in Figures 2, 3 and 4. The LEP average values are given in Table 4.

Three-Parameter Analyses

The results from each experiment are shown in Table 5, where the uncertainties include both statistical and systematic effects. The LEP average values are given in Table 6.

5.2 Neutral Triple Gauge Boson Couplings in $Z\gamma$ Production

Single-Parameter Analyses

The results from each experiment are shown in Table 7, where the uncertainties include both statistical and systematic effects. The individual $\log \mathcal{L}$ curves and their sum are shown in Figures 5 and 6. The results of the combination are given in Table 8.

Two-Parameter Analyses

The results from each experiment are shown in Table 9, where the uncertainties include both statistical and systematic effects. The 68% C.L. and 95% C.L. contours curves resulting from

the combinations of the two-dimensional likelihood curves are shown in Figures 7, 8, 9, and 10. The LEP average values are given in Table 10.

5.3 Neutral Triple Gauge Boson Couplings in ZZ Production

Single-Parameter Analyses

The results from each experiment are shown in Table 11, where the uncertainties include both statistical and systematic effects. The individual $\log \mathcal{L}$ curves and their sum are shown in Figure 11. The results of the combination are given in Table 12.

Two-Parameter Analyses

The results from each experiment are shown in Table 13, where the uncertainties include both statistical and systematic effects. The 68% C.L. and 95% C.L. contours curves resulting from the combinations of the two-dimensional likelihood curves are shown in Figures 12 and 13. The LEP average values are given in Table 14.

5.4 Quartic Gauge Boson Couplings

The results from each experiment are shown in Table 15, where the uncertainties include both statistical and systematic effects. The individual $\log \mathcal{L}$ curves and their sum are shown in Figures 14 and 15. The results of the combination are given in Table 16.

Conclusions

The existence of triple gauge boson couplings among the electroweak gauge bosons is experimentally verified. No significant deviation from the Standard Model predictions is seen for any of the electroweak gauge boson couplings investigated. As an example, these data allow the Kaluza-Klein theory [28], in which $\kappa_\gamma = -2$, to be excluded completely [29].

Acknowledgements

We would like to thank the CERN accelerator divisions for the efficient operation of the LEP accelerator.

Parameter	ALEPH [2]	DELPHI [3]	L3 [4]	OPAL [5]
g_5^{Z}	$+0.13^{+0.21}_{-0.21}$	—	$-0.04^{+0.24}_{-0.25}$	—
Δg_1^{Z}	$+0.008^{+0.040}_{-0.039}$	$-0.028^{+0.046}_{-0.045}$	$-0.075^{+0.058}_{-0.054}$	$-0.046^{+0.043}_{-0.041}$
$\Delta\kappa_\gamma$	$+0.04^{+0.09}_{-0.09}$	$+0.05^{+0.13}_{-0.12}$	$-0.03^{+0.12}_{-0.11}$	$-0.10^{+0.11}_{-0.10}$
λ_γ	$-0.012^{+0.041}_{-0.039}$	$+0.056^{+0.057}_{-0.056}$	$-0.081^{+0.065}_{-0.058}$	$-0.108^{+0.040}_{-0.038}$

Table 1: The measured central values and one standard deviation uncertainties ($\Delta \log \mathcal{L} = 0.5$) obtained by the four LEP experiments. In each case the parameter listed is varied while the remaining ones are fixed to their Standard Model value. Both statistical and systematic uncertainties are included.

Parameter	68% C.L.	95% C.L.
g_5^{Z}	$+0.05^{+0.16}_{-0.17}$	$[-0.28, \quad +0.36]$
Δg_1^{Z}	$-0.025^{+0.026}_{-0.026}$	$[-0.074, \quad +0.028]$
$\Delta\kappa_\gamma$	$-0.002^{+0.067}_{-0.065}$	$[-0.13, \quad +0.13]$
λ_γ	$-0.036^{+0.028}_{-0.027}$	$[-0.089, \quad +0.020]$

Table 2: The central values, 68% C.L. uncertainties and 95% C.L. intervals ($\Delta \log \mathcal{L} = 0.5,\ 1.92$) obtained combining the results from the four LEP experiments. In each case the parameter listed is varied while the remaining ones are fixed to their Standard Model value. Both statistical and systematic uncertainties are included.

Parameter	ALEPH [2]	DELPHI [3]	L3 [4]	OPAL [5]
Δg_1^{Z}	$-0.001^{+0.043}_{-0.045}$	$-0.048^{+0.049}_{-0.046}$	$-0.088^{+0.095}_{-0.064}$	$-0.017^{+0.049}_{-0.061}$
$\Delta\kappa_\gamma$	$+0.02^{+0.09}_{-0.09}$	$+0.14^{+0.11}_{-0.11}$	$+0.04^{+0.13}_{-0.17}$	$-0.11^{+0.17}_{-0.10}$
Δg_1^{Z}	$+0.019^{+0.052}_{-0.051}$	$-0.103^{+0.063}_{-0.058}$	$-0.02^{+0.10}_{-0.16}$	$+0.075^{+0.059}_{-0.059}$
λ_γ	$-0.026^{+0.053}_{-0.055}$	$+0.111^{+0.069}_{-0.072}$	$-0.06^{+0.19}_{-0.10}$	$-0.158^{+0.054}_{-0.051}$
λ_γ	$-0.019^{+0.044}_{-0.044}$	$+0.032^{+0.060}_{-0.058}$	$-0.088^{+0.093}_{-0.067}$	$-0.103^{+0.044}_{-0.044}$
$\Delta\kappa_\gamma$	$+0.03^{+0.09}_{-0.09}$	$+0.07^{+0.11}_{-0.10}$	$+0.03^{+0.12}_{-0.14}$	$-0.03^{+0.14}_{-0.11}$

Table 3: The measured central values and one standard deviation uncertainties ($\Delta \log \mathcal{L} = 0.5$) obtained by the four LEP experiments. In each case the two parameters listed are varied while the remaining one is fixed to its Standard Model value. Both statistical and systematic uncertainties are included.

Parameter	68% C.L.	95% C.L.	Correlations	
Δg_1^{Z}	$-0.038^{+0.041}_{-0.034}$	$[-0.10, +0.03]$	1.00	-0.43
$\Delta\kappa_\gamma$	$+0.053^{+0.074}_{-0.089}$	$[-0.10, +0.21]$	-0.43	1.00
Δg_1^{Z}	$+0.006^{+0.035}_{-0.039}$	$[-0.072, +0.076]$	1.00	-0.70
λ_γ	$-0.048^{+0.043}_{-0.036}$	$[-0.12, +0.03]$	-0.70	1.00
λ_γ	$-0.046^{+0.041}_{-0.031}$	$[-0.11, +0.02]$	1.00	-0.19
$\Delta\kappa_\gamma$	$+0.037^{+0.060}_{-0.069}$	$[-0.09, +0.16]$	-0.19	1.00

Table 4: The central values, 68% C.L. uncertainties and 95% C.L. intervals ($\Delta \log \mathcal{L} = 0.5,\ 1.92$) obtained combining the results from the four LEP experiments. In each case the two parameters listed are varied while the remaining one is fixed to its Standard Model value. Both statistical and systematic uncertainties are included. Since the shape of the log-likelihood is not parabolic, there is some ambiguity in the definition of the correlation coefficients and the values quoted here are approximate.

Parameter	ALEPH [2]	L3 [4]	OPAL [5]
Δg_1^{Z}	$+0.018^{+0.043}_{-0.043}$	$-0.02^{+0.11}_{-0.18}$	$+0.081^{+0.054}_{-0.058}$
$\Delta\kappa_\gamma$	$+0.013^{+0.071}_{-0.071}$	$-0.02^{+0.14}_{-0.15}$	$-0.07^{+0.11}_{-0.09}$
λ_γ	$-0.028^{+0.044}_{-0.047}$	$-0.07^{+0.21}_{-0.11}$	$-0.149^{+0.055}_{-0.053}$

Table 5: The measured central values and one standard deviation uncertainties ($\Delta \log \mathcal{L} = 0.5$) obtained by ALEPH, L3 and OPAL. All three parameters listed are varied. Both statistical and systematic uncertainties are included.

Parameter	68% C.L.	95% C.L.	Correlations		
Δg_1^{Z}	$+0.023^{+0.039}_{-0.041}$	$[-0.06, +0.10]$	1.00	-0.20	-0.66
$\Delta\kappa_\gamma$	$+0.027^{+0.073}_{-0.072}$	$[-0.11, +0.18]$	-0.20	1.00	-0.15
λ_γ	$-0.067^{+0.044}_{-0.037}$	$[-0.14, +0.02]$	-0.66	-0.15	1.00

Table 6: The central values, 68% C.L. uncertainties and 95% C.L. intervals ($\Delta \log \mathcal{L} = 0.5,\ 1.92$) obtained combining the results from ALEPH, L3 and OPAL. All three parameters listed are varied. Both statistical and systematic uncertainties are included. Since the shape of the log-likelihood is not parabolic, there is some ambiguity in the definition of the correlation coefficients and the values quoted here are approximate.

Parameter	DELPHI [6]	L3 [7]	OPAL [8]
h_1^γ	$[-0.17, \ +0.17]$	$[-0.14, \ +0.03]$	$[-0.11, \ +0.11]$
h_2^γ	$[-0.11, \ +0.11]$	$[-0.039, \ +0.079]$	$[-0.077, \ +0.077]$
h_3^γ	$[-0.058, \ +0.051]$	$[-0.095, \ -0.001]$	$[-0.17, \ -0.01]$
h_4^γ	$[-0.036, \ +0.041]$	$[+0.005, \ +0.072]$	$[+0.01, \ +0.14]$
h_1^Z	$[-0.28, \ +0.29]$	$[-0.16, \ +0.04]$	$[-0.19, \ +0.19]$
h_2^Z	$[-0.18, \ +0.18]$	$[-0.042, \ +0.093]$	$[-0.13, \ +0.13]$
h_3^Z	$[-0.37, \ +0.21]$	$[-0.16, \ +0.11]$	$[-0.27, \ +0.12]$
h_4^Z	$[-0.14, \ +0.22]$	$[-0.05, \ +0.11]$	$[-0.08, \ +0.18]$

Table 7: The 95% C.L. intervals ($\Delta \log \mathcal{L} = 1.92$) measured by DELPHI, L3 and OPAL. In each case the parameter listed is varied while the remaining ones are fixed to their Standard Model value. Both statistical and systematic uncertainties are included.

Parameter	95% C.L.
h_1^γ	$[-0.10, \ +0.03]$
h_2^γ	$[-0.036, \ +0.061]$
h_3^γ	$[-0.075, \ -0.004]$
h_4^γ	$[+0.005, \ +0.056]$
h_1^Z	$[-0.13, \ +0.04]$
h_2^Z	$[-0.041, \ +0.080]$
h_3^Z	$[-0.16, \ +0.07]$
h_4^Z	$[-0.04, \ +0.10]$

Table 8: The 95% C.L. intervals ($\Delta \log \mathcal{L} = 1.92$) obtained combining the results from DELPHI, L3 and OPAL. In each case the parameter listed is varied while the remaining ones are fixed to their Standard Model value. Both statistical and systematic uncertainties are included.

Parameter	DELPHI [6]	L3 [7]
h_1^γ	$[-0.35, +0.35]$	$[-0.23, +0.10]$
h_2^γ	$[-0.23, +0.23]$	$[-0.12, +0.10]$
h_3^γ	$[-0.26, +0.38]$	$[-0.20, +0.12]$
h_4^γ	$[-0.32, +0.43]$	$[-0.10, +0.12]$
h_1^Z	$[-0.58, +0.58]$	$[-0.49, +0.19]$
h_2^Z	$[-0.38, +0.38]$	$[-0.31, +0.16]$
h_3^Z	$[-0.70, +0.50]$	$[-0.37, +0.40]$
h_4^Z	$[-0.41, +0.37]$	$[-0.20, +0.28]$

Table 9: The 95% C.L. intervals ($\Delta \log \mathcal{L} = 1.92$) measured by DELPHI and L3. In each case the two parameters listed are varied while the remaining ones are fixed to their Standard Model value. Both statistical and systematic uncertainties are included.

Parameter	95% C.L.	Correlations	
h_1^γ	$[-0.21, +0.10]$	1.00	+0.88
h_2^γ	$[-0.11, +0.10]$	+0.88	1.00
h_3^γ	$[-0.20, +0.13]$	1.00	+0.98
h_4^γ	$[-0.11, +0.12]$	+0.98	1.00
h_1^Z	$[-0.44, +0.20]$	1.00	+0.96
h_2^Z	$[-0.28, +0.16]$	+0.96	1.00
h_3^Z	$[-0.38, +0.35]$	1.00	+0.95
h_4^Z	$[-0.21, +0.26]$	+0.95	1.00

Table 10: The 95% C.L. intervals ($\Delta \log \mathcal{L} = 1.92$) obtained combining the results from DELPHI and L3. In each case the two parameters listed are varied while the remaining ones are fixed to their Standard Model value. Both statistical and systematic uncertainties are included. Since the shape of the log-likelihood is not parabolic, there is some ambiguity in the definition of the correlation coefficients and the values quoted here are approximate.

Parameter	DELPHI [9]	L3 [10]	OPAL [11]
f_4^γ	$[-0.49, \ +0.49]$	$[-0.59, \ +0.58]$	$[-0.45, \ +0.43]$
f_4^Z	$[-0.82, \ +0.83]$	$[-0.97, \ +0.99]$	$[-0.74, \ +0.75]$
f_5^γ	$[-1.2, \ +1.2]$	$[-1.4, \ +1.4]$	$[-0.9, \ +0.8]$
f_5^Z	$[-1.9, \ +2.1]$	$[-2.2, \ +2.5]$	$[-1.0, \ +0.5]$

Table 11: The 95% C.L. intervals ($\Delta \log \mathcal{L} = 1.92$) measured by DELPHI, L3 and OPAL. In each case the parameter listed is varied while the remaining ones are fixed to their Standard Model value. Both statistical and systematic uncertainties are included.

Parameter	95% C.L.
f_4^γ	$[-0.41, \ +0.39]$
f_4^Z	$[-0.66, \ +0.68]$
f_5^γ	$[-0.89, \ +0.84]$
f_5^Z	$[-1.1, \ +0.5]$

Table 12: The 95% C.L. intervals ($\Delta \log \mathcal{L} = 1.92$) obtained combining the results from DELPHI, L3 and OPAL. In each case the parameter listed is varied while the remaining ones are fixed to their Standard Model value. Both statistical and systematic uncertainties are included.

Parameter	DELPHI [9]	L3 [10]	OPAL [11]
f_4^γ	$[-0.49, \ +0.49]$	$[-0.58, \ +0.58]$	$[-0.45, \ +0.43]$
f_4^Z	$[-0.82, \ +0.83]$	$[-0.97, \ +0.99]$	$[-0.73, \ +0.75]$
f_5^γ	$[-1.2, \ +1.2]$	$[-1.4, \ +1.4]$	$[-0.9, \ +0.9]$
f_5^Z	$[-1.9, \ +2.1]$	$[-2.2, \ +2.5]$	$[-1.0, \ +0.7]$

Table 13: The 95% C.L. intervals ($\Delta \log \mathcal{L} = 1.92$) measured by DELPHI, L3 and OPAL. In each case the two parameters listed are varied while the remaining ones are fixed to their Standard Model value. Both statistical and systematic uncertainties are included.

Parameter	95% C.L.	Correlations	
f_4^γ	$[-0.40, \ +0.38]$	1.00	+0.88
f_4^Z	$[-0.66, \ +0.68]$	+0.88	1.00
f_5^γ	$[-0.88, \ +0.86]$	1.00	−0.52
f_5^Z	$[-1.1, \ +0.7]$	−0.52	1.00

Table 14: The 95% C.L. intervals ($\Delta \log \mathcal{L} = 1.92$) obtained combining the results from DELPHI, L3 and OPAL. In each case the two parameters listed are varied while the remaining ones are fixed to their Standard Model value. Both statistical and systematic uncertainties are included. Since the shape of the log-likelihood is not parabolic, there is some ambiguity in the definition of the correlation coefficients and the values quoted here are approximate.

Parameter [GeV^{-2}]	ALEPH [12]	L3 [13]	OPAL [14]
a_0/Λ^2	$[-0.043, \ +0.042]$	$[-0.036, \ +0.035]$	$[-0.065, \ +0.0065]$
a_c/Λ^2	$[-0.11, \ +0.11]$	$[-0.08, \ +0.11]$	$[-0.13, \ +0.17]$
a_n/Λ^2	—	$[-0.45, \ +0.42]$	$[-0.61, \ +0.57]$
a_0/Λ^2	—	$[-0.006, \ +0.006]$	$[-0.006, \ +0.008]$
a_c/Λ^2	—	$[-0.006, \ +0.010]$	$[-0.008, \ +0.012]$

Table 15: The 95% C.L. intervals ($\Delta \log \mathcal{L} = 1.92$) measured by ALEPH, L3 and OPAL. In each case the parameter listed is varied while the remaining ones are fixed to their Standard Model value. Both statistical and systematic uncertainties are included. Top: WWγ and $\nu\bar{\nu}\gamma\gamma$. Bottom: Z$\gamma\gamma$.

Parameter [GeV^{-2}]	95% C.L.
a_0/Λ^2	$[-0.037, \ +0.036]$
a_c/Λ^2	$[-0.077, \ +0.095]$
a_n/Λ^2	$[-0.45, \ +0.41]$
a_0/Λ^2	$[-0.0048, \ +0.0056]$
a_c/Λ^2	$[-0.0052, \ +0.0099]$

Table 16: The 95% C.L. intervals ($\Delta \log \mathcal{L} = 1.92$) obtained combining the results from ALEPH, L3 and OPAL. In each case the parameter listed is varied while the remaining ones are fixed to their Standard Model value. Both statistical and systematic uncertainties are included. Top: WWγ and $\nu\bar{\nu}\gamma\gamma$. Bottom: Z$\gamma\gamma$.

A Correlated Systematic Uncertainties

The systematic uncertainties on charged TGCs for each source considered as correlated between experiments are reported in Table 17. For each systematic source considered, the corresponding uncertainty on a given TGC is averaged over the contributing measurements weighted by the uncorrelated uncertainty of the measurement as derived from its 68% C.L. range. The average systematic uncertainty due to each source is then added in quadrature to yield the total correlated uncertainty, and thus the scale factor for the TGC under consideration. For multi-parameter analyses, the unweighted average of the scale factors of the TGCs varied in the respective analysis is used. This procedure is applied separately for results derived from W-pair and from single-W production; the results from these two processes on charged TGCs are treated as uncorrelated in the combination. Further studies on correlated systematic uncertainties and the combination procedure are currently under way.

Δg_1^Z					
Experiment	theo	frag	BE	CR	theo
ALEPH	0.015	0.016	0.005	0.000	0.000
DELPHI	0.006	0.002	0.005	0.006	0.018
L3	0.020	0.008	0.008	0.008	0.000
OPAL	0.005	0.009	0.003	0.002	0.000
$\Delta\kappa_\gamma$					
Experiment	theo	frag	BE	CR	theo
ALEPH	0.06	0.06	0.01	0.01	0.05
DELPHI	0.062	0.033	0.020	0.022	0.071
L3	0.067	0.037	0.036	0.019	0.041
OPAL	0.038	0.022	0.005	0.001	0.051
λ_γ					
Experiment	theo	frag	BE	CR	theo
ALEPH	0.015	0.015	0.004	0.005	0.07
DELPHI	0.019	0.006	0.002	0.002	0.021
L3	0.020	0.010	0.009	0.009	0.094
OPAL	0.008	0.006	0.002	0.002	0.073
g_5^Z					
Experiment	theo	frag	BE	CR	theo
ALEPH	0.004	0.051	0.000	0.000	—
L3	0.056	0.050	0.077	0.044	—

Table 17: Sources of systematic uncertainties considered as correlated between experiments (theoretical cross section uncertainty, fragmentation, Bose-Einstein correlations and colour reconnection effects in W-pair production; and theoretical cross section uncertainty in single-W production).

References

[1] G. Gounaris *et al.*, in *Physics at LEP 2*, Report CERN 96-01 (1996), eds G. Altarelli, T. Sjöstrand, F. Zwirner, Vol. 1, p. 525.

[2] The ALEPH Collaboration, R. Barate *et al.*, Phys. Lett. **B 422** (1998) 369;
The ALEPH Collaboration, *Measurement of Triple Gauge-Boson Couplings at LEP energies up to 189 GeV*, ICHEP 2000 abstract 324;
The ALEPH Collaboration, *Single W Production at Energies up to* $\sqrt{s}$ *= 202 GeV and Search for Anomalous Triple Gauge Boson Couplings*, ICHEP 2000 abstract 304;
The ALEPH Collaboration, *Measurement of Triple Gauge-Boson Couplings at 192-202 GeV*, ICHEP 2000 abstract 302.

[3] The DELPHI Collaboration, P. Abreu *et al.*, Phys. Lett. **B 397** (1997) 158;
The DELPHI Collaboration, P. Abreu *et al.*, Phys. Lett. **B 423** (1998) 194;
The DELPHI Collaboration, *Measurement of Trilinear* $WW\gamma$ *and WWZ Gauge Boson Couplings at values of* $\sqrt{s}$ *from 183 to 202 GeV* , ICHEP 2000 abstract 457.

[4] The L3 Collaboration, M. Acciari *et al.*, Phys. Lett. **B 398** (1997) 223;
The L3 Collaboration, M. Acciari *et al.*, Phys. Lett. **B 413** (1998) 176;
The L3 Collaboration, M. Acciari *et al.*, Phys. Lett. **B 467** (1999) 171;
The L3 Collaboration, *Preliminary Results on the Measurement of Triple-Gauge-Boson Couplings of the W Boson at LEP*, L3 Note 2567 (6/2000), ICHEP 2000 abstract 524.

[5] The OPAL Collaboration, K. Ackerstaff *et al.*, Phys. Lett. **B 397** (1997) 147;
The OPAL Collaboration, K. Ackerstaff *et al.*, Eur. Phys. J. **C 2** (1998) 597;
The OPAL Collaboration, G. Abbiendi *et al.*, Eur. Phys. J. C9 (1999) 191;
The OPAL Collaboration, G. Abbiendi *et al.*, CERN-EP/2000-114, submitted to Eur. Phys. J. **C**;
The OPAL Collaboration, *Triple gauge boson couplings in* W^+W^- *production at LEP energies up to 202 GeV*, OPAL physics note PN441 (7/2000), ICHEP 2000 abstract 206;
The OPAL Collaboration, *Measurement of Single W production and Triple Gauge Couplings in* e^+e^- *Collisions at* $\sqrt{s}$ *=189 GeV*, OPAL physics note PN427 (3/2000), ICHEP 2000 abstract 148.

[6] The DELPHI Collaboration, *Study of Trilinear Gauge Boson Couplings* $ZZ\gamma$ *and* $Z\gamma\gamma$ *between 189 and 202 GeV*, ICHEP 2000 abstract 456.

[7] The L3 Collaboration, M. Acciari *et al.*, Phys. Lett. **B 436** (1999) 187;
The L3 Collaboration, M. Acciari *et al.*, CERN-EP/2000-057, accepted by Phys. Lett. **B**;
The L3 Collaboration, *Study of anomalous* $ZZ\gamma$ *and* $Z\gamma\gamma$ *couplings at LEP*, L3 Note 2552 (6/2000), ICHEP 2000 abstract 504.

[8] The OPAL Collaboration, G. Abbiendi *et al.*, CERN-EP/2000-067, accepted by Eur. Phys. J. **C**.

[9] The DELPHI Collaboration, *Measurement of ZZ production using data between* $\sqrt{s}$ *=183 and 202 GeV*, ICHEP 2000 abstract 659.

[10] The L3 Collaboration, M. Acciari *et al.*, Phys. Lett. **B 450** (1999) 281;
The L3 Collaboration, M. Acciari *et al.*, Phys. Lett. **B 465** (1999) 363;
The L3 Collaboration, *Study of Z Boson Pair Production at LEP*, L3 Note 2579 (7/2000), ICHEP 2000 abstract 502.

[11] The OPAL Collaboration, G. Abbiendi *et al.*, Phys. Lett. **B476** (2000) 256;
The OPAL Collaboration, *Z boson pair production in e^+e^- collisions at $\sqrt{s} > 190$ GeV*, OPAL physics note PN423 (3/2000), ICHEP 2000 abstract 154;
The OPAL Collaboration, *Measurement of Standard Model Processes in e^+e^- collisions at $\sqrt{s} > 202$ GeV*, OPAL physics note PN437 (7/2000), ICHEP 2000 abstract 168.

[12] The ALEPH Collaboration, *Constraints on Anomalous Quartic Gauge Boson Couplings from $e^+e^- \to \nu\bar{\nu}\gamma\gamma(\gamma)$ at 189-202 GeV*, ICHEP 2000 abstract 286.

[13] The L3 Collaboration, M. Acciari *et al.*, Phys. Lett. **B 478** (2000) 39;
The L3 Collaboration, *Measurement of the $e^+e^- \to Z\gamma\gamma$ Cross Section and Study of Anomalous Quartic Gauge Couplings*, L3 Note 2578 (7/2000), ICHEP 2000 abstract 505;
The L3 Collaboration, *Preliminary Measurement of the $W^+W^-\gamma$ Cross Section and direct Limits on Anomalous Quartic Gauge Boson Couplings at LEP*, (includes $\nu\bar{\nu}\gamma\gamma(\gamma)$), L3 Note 2569 (7/2000), ICHEP 2000 abstract 520.

[14] The OPAL Collaboration, G. Abbiendi *et al.*, Phys. Lett. **B 471** (1999) 293;
The OPAL Collaboration, *Constraints on anomalous quartic gauge boson couplings from acoplanar photon pair events*, OPAL physics note PN410 (7/1999), EPS 1999 abstract 6-353;
The OPAL Collaboration, *Measurement of the $e^+e^- \to q\overline{q}\gamma\gamma$ cross section and limits on anomalous electroweak quartic gauge couplings*, OPAL physics note PN452 (7/2000), ICHEP 2000 abstract 572.

[15] K. Gaemers and G. Gounaris, Z. Phys. **C 1** (1979) 259.

[16] K. Hagiwara, K. Hikasa, R.D. Peccei and D. Zeppenfeld, Nucl. Phys. **B 282** (1987) 253.

[17] K. Hagiwara, S. Ishihara, R. Szalapski, and D. Zeppenfeld, Phys. Lett. **B 283** (1992) 353;
K. Hagiwara, S. Ishihara, R. Szalapski, and D. Zeppenfeld, Phys. Rev. **D 48** (1993) 2182;
K. Hagiwara, T. Hatsukano, S. Ishihara and R. Szalapski, Nucl. Phys. **B 496** (1997) 66.

[18] M. Bilenky, J.L. Kneur, F.M. Renard and D. Schildknecht, Nucl. Phys. **B 409** (1993) 22;
M. Bilenky, J.L. Kneur, F.M. Renard and D. Schildknecht, Nucl. Phys. **B 419** (1994) 240.

[19] I. Kuss and D. Schildknecht, Phys. Lett. **B 383** (1996) 470.

[20] G. Gounaris and C.G. Papadopoulos, Eur. Phys. J. **C 2** (1998) 365.

[21] G. J. Gounaris, J. Layssac and F. M. Renard, Phys. Rev. **D 61** (2000) 073013.

[22] G. Bélanger and F. Boudjema, Phys. Lett. **B 288** (1992) 201.

[23] W. J. Stirling and A. Werthenbach, Eur. Phys. J. **C 14** (2000) 103.

[24] W. J. Stirling and A. Werthenbach, Phys. Lett. **B 466** (1999) 369.

[25] G. Bélanger *et al.*, Eur. Phys. J. **C 13** (2000) 283.

[26] The LEP electroweak working group, Preprint CERN-EP/2000-016, January 2000.

[27] The LEP-TGC combination group, LEPEWWG/TGC/2000-01, March 2000.

[28] O.Klein, *On the Theory of Charged Fields*, New Theories in Physics, Proceedings, Warsaw, 1938; reprinted in: Surveys of High Energ. Phys. **5** (1986) 269.

[29] L.Maiani and P.M.Zerwas, *W Static ELM Parameters*, Memorandum to the TGC Combination Group (1998).

The physics notes describing the preliminary results of the LEP experiments submitted to the summer conferences 2000 are available on the world-wide web at:

ALEPH:	`http://alephwww.cern.ch/ALPUB/oldconf/osaka00/osaka.html`
DELPHI:	`http://delphiwww.cern.ch/~pubxx/delwww/www/delsec/conferences/osaka/`
L3:	`http://l3www.cern.ch/conferences/Osaka2000/index.html`
OPAL:	`http://opal.web.cern.ch/Opal/pubs/ichep2000/abstract/abstr.html`

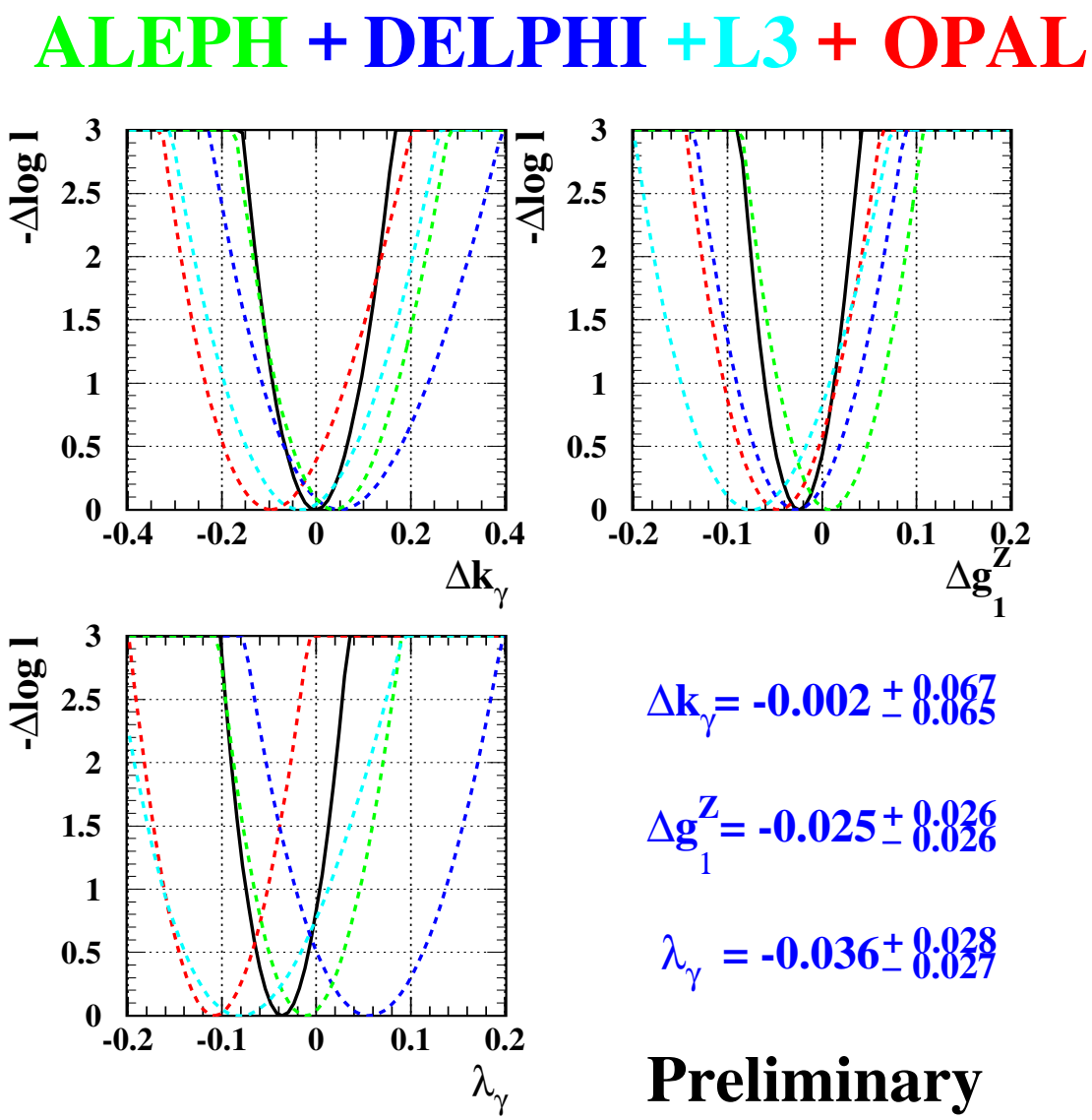

Figure 1: The $\log \mathcal{L}$ curves of the four experiments (dashed lines) and the LEP combined curve (solid line) for the three charged TGCs Δg_1^Z, $\Delta\kappa_\gamma$ and λ_γ. In each case, the minimal value is subtracted.

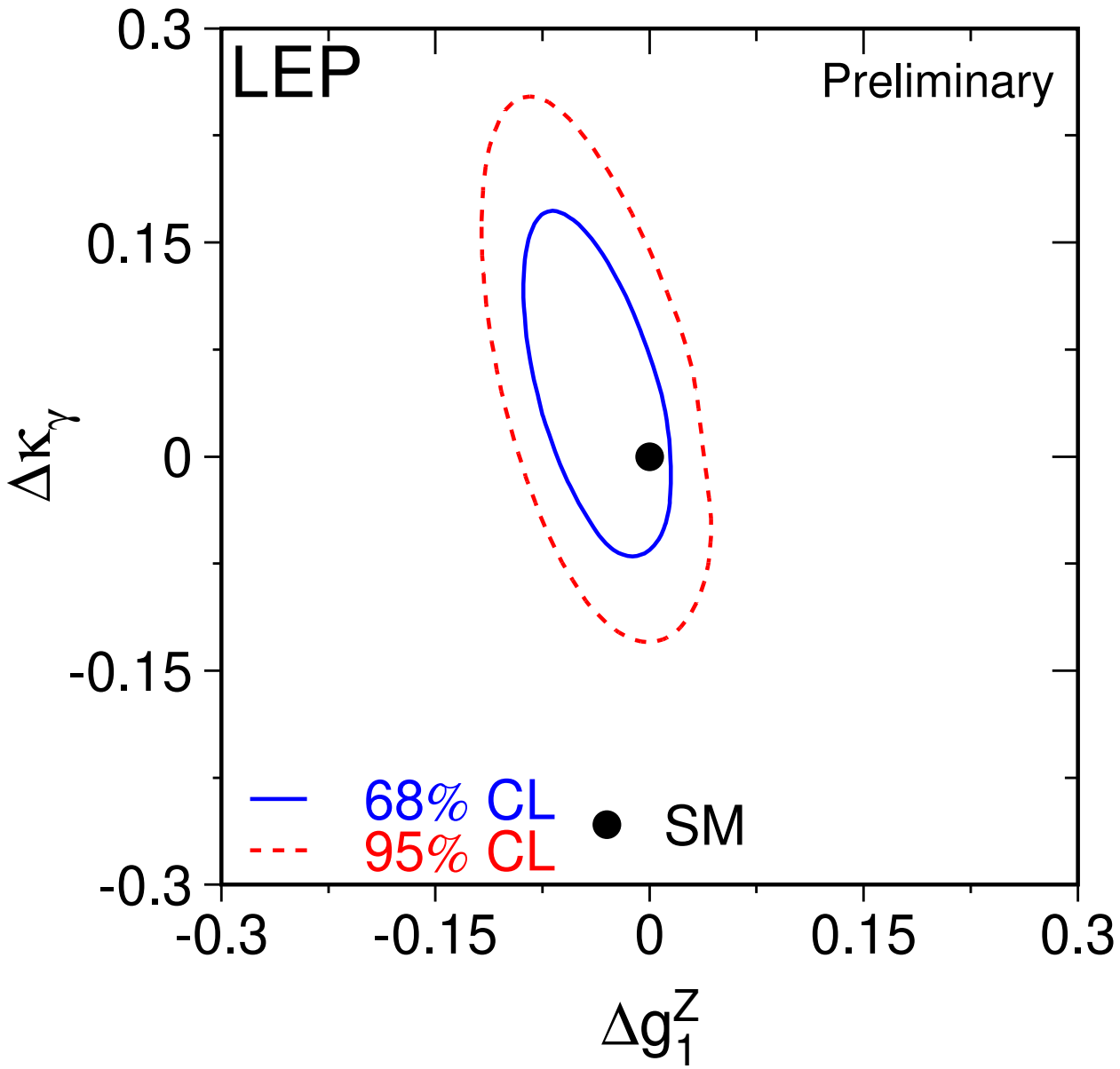

Figure 2: Contour curves of 68% C.L. and 95% C.L. in the plane $(\Delta g_1^Z, \Delta\kappa_\gamma)$ showing the LEP combined result.

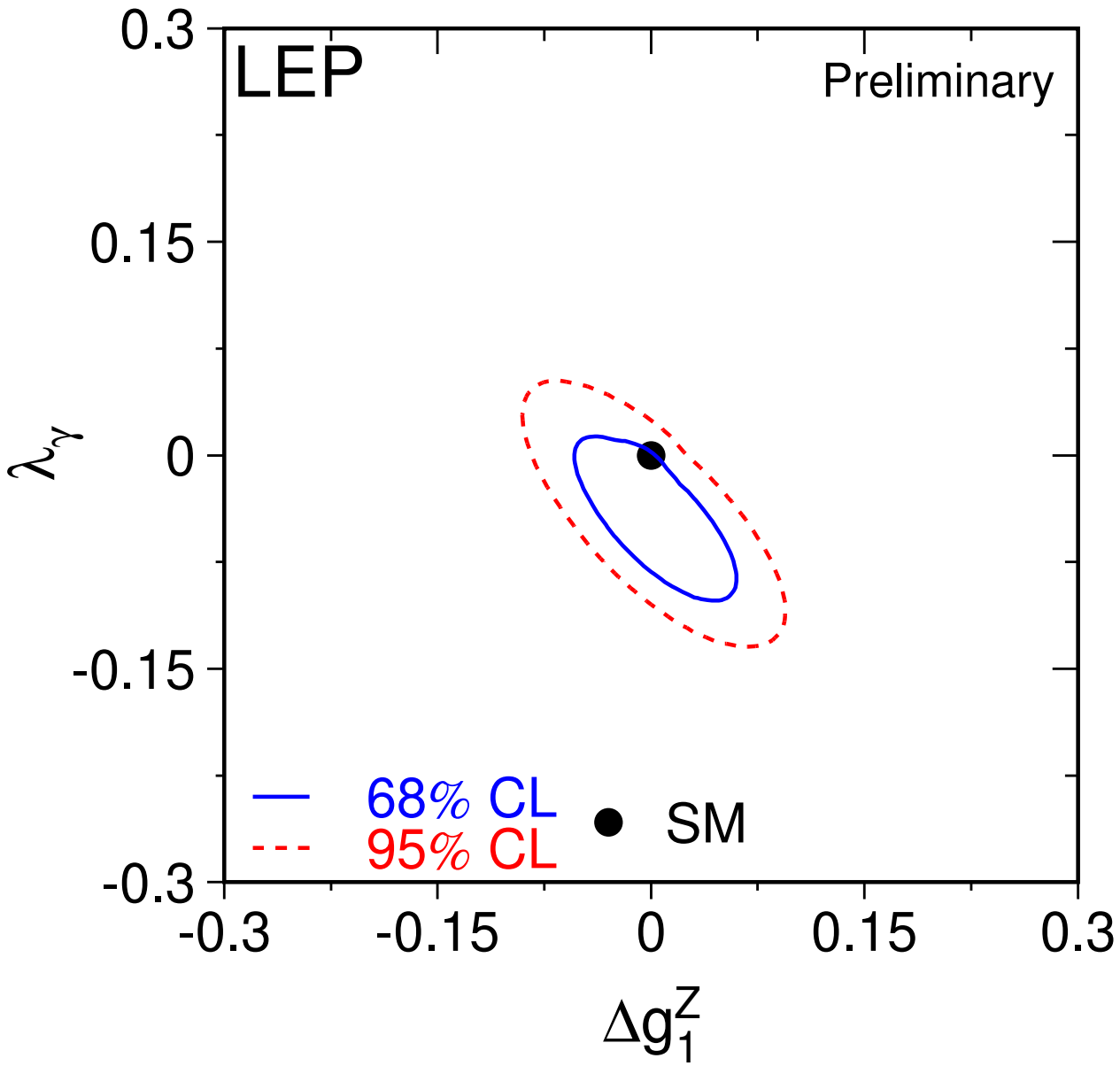

Figure 3: Contour curves of 68% C.L. and 95% C.L. in the plane $(\Delta g_1^Z, \lambda_\gamma)$ showing the LEP combined result.

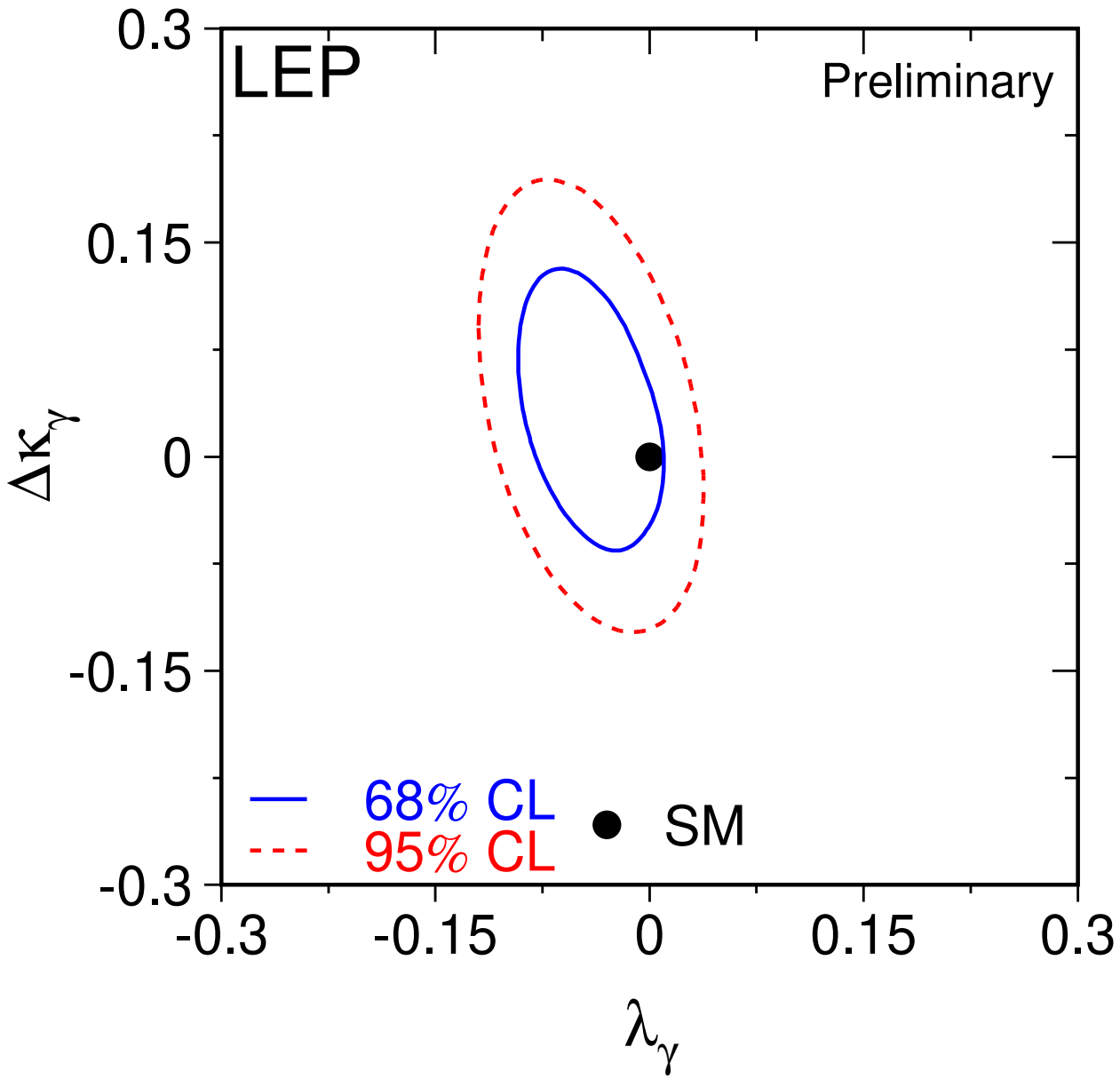

Figure 4: Contour curves of 68% C.L. and 95% C.L. in the plane $(\lambda_\gamma, \Delta\kappa_\gamma)$ showing the LEP combined result.

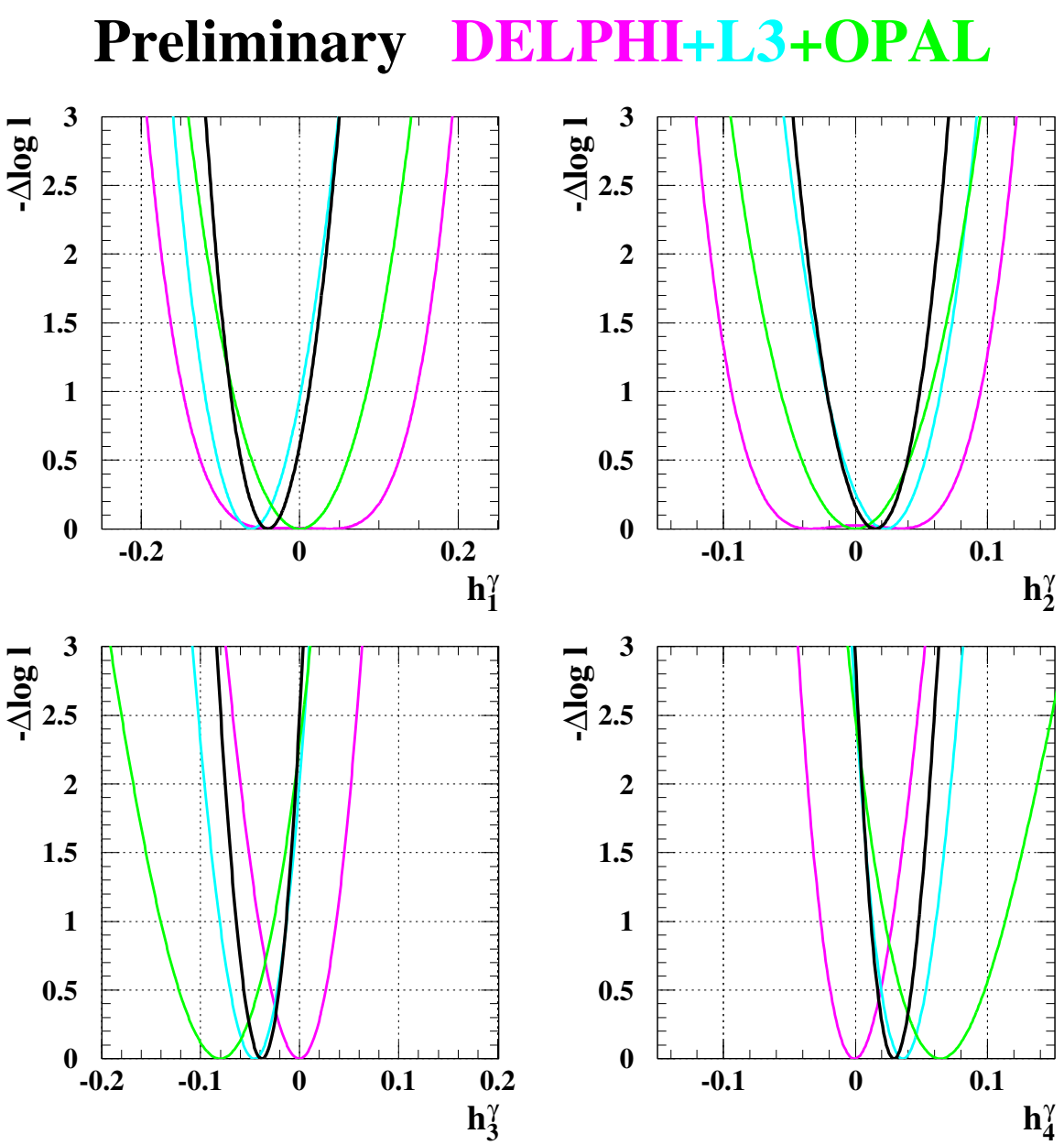

Figure 5: The $\log \mathcal{L}$ curves of DELPHI, L3 and OPAL, and the LEP combined curve for the four neutral TGCs h_i^γ, $i = 1, 2, 3, 4$. In each case, the minimal value is subtracted.

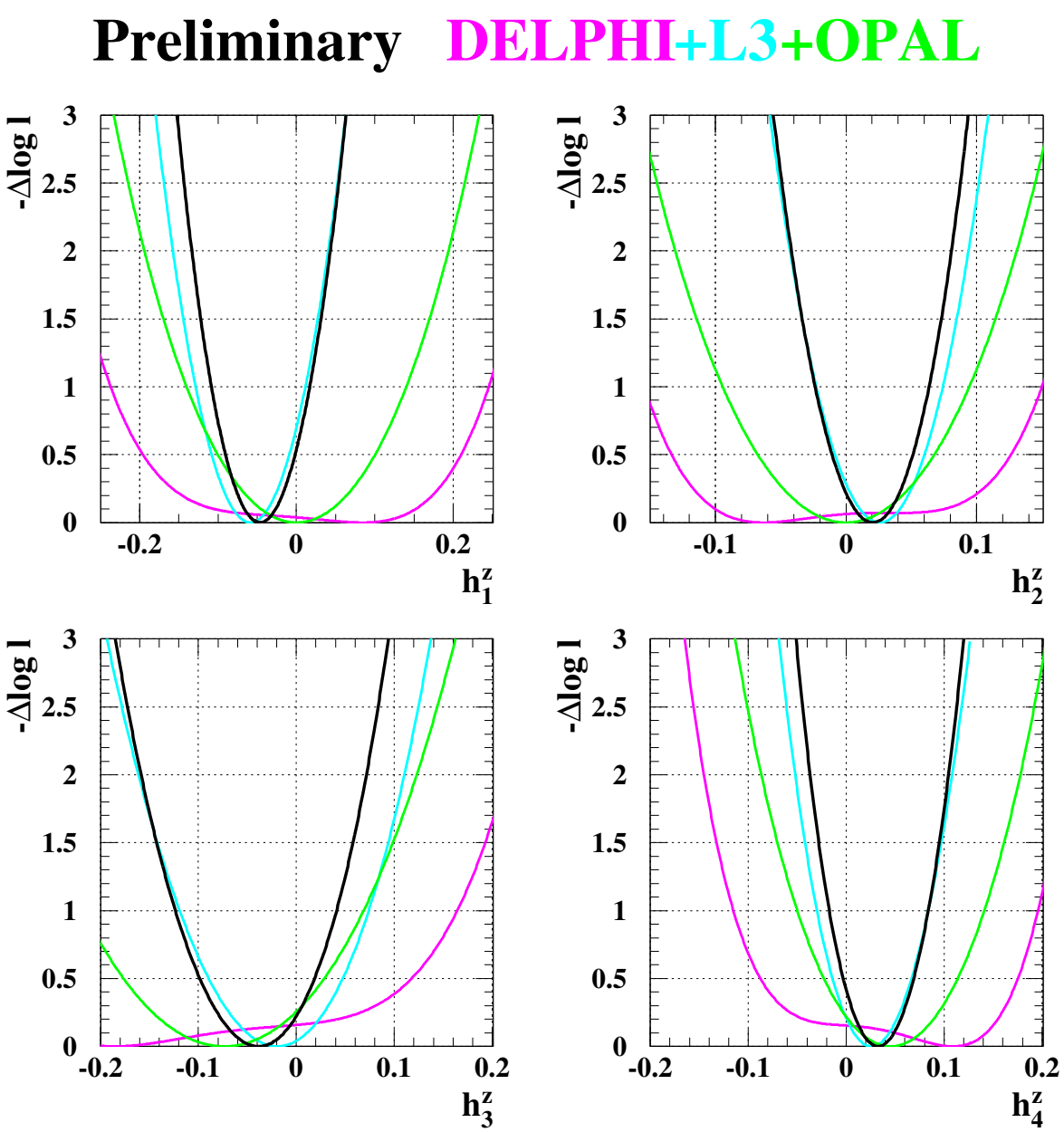

Figure 6: The $\log \mathcal{L}$ curves of DELPHI, L3 and OPAL, and the LEP combined curve for the four neutral TGCs h_i^Z, $i = 1, 2, 3, 4$. In each case, the minimal value is subtracted.

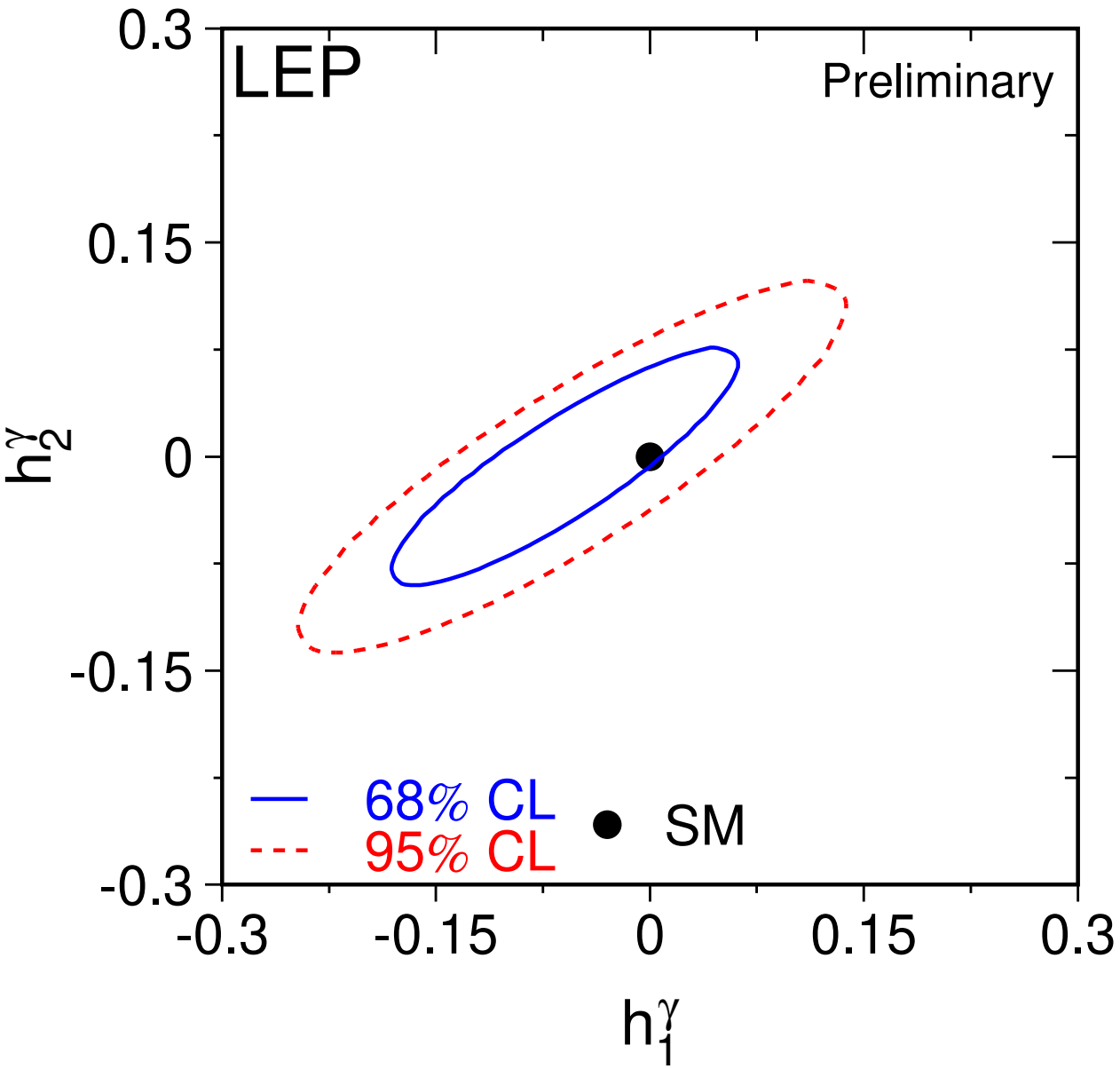

Figure 7: Contour curves of 68% C.L. and 95% C.L. in the plane (h_1^γ, h_2^γ) showing the LEP combined result.

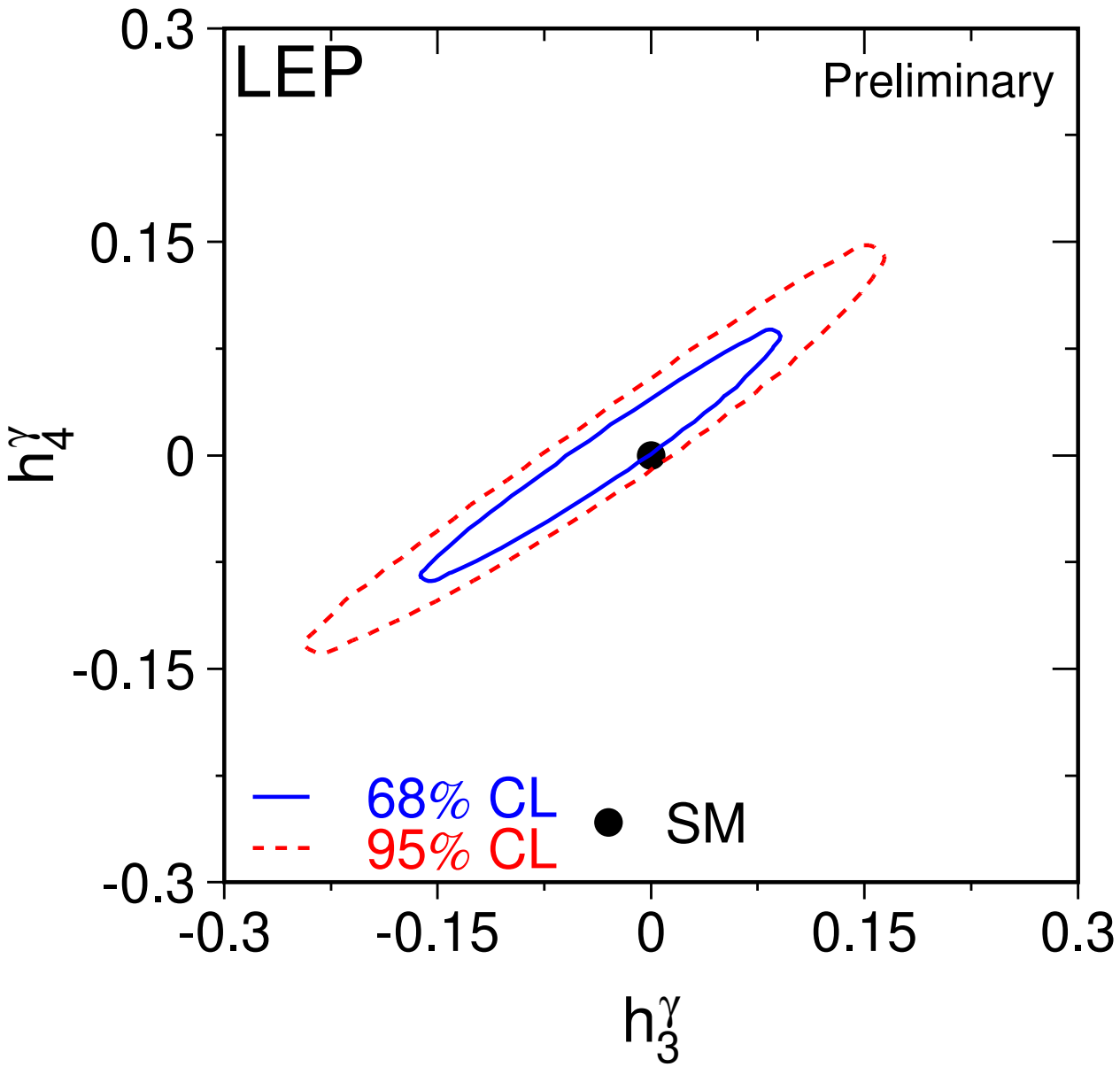

Figure 8: Contour curves of 68% C.L. and 95% C.L. in the plane (h_3^γ, h_4^γ) showing the LEP combined result.

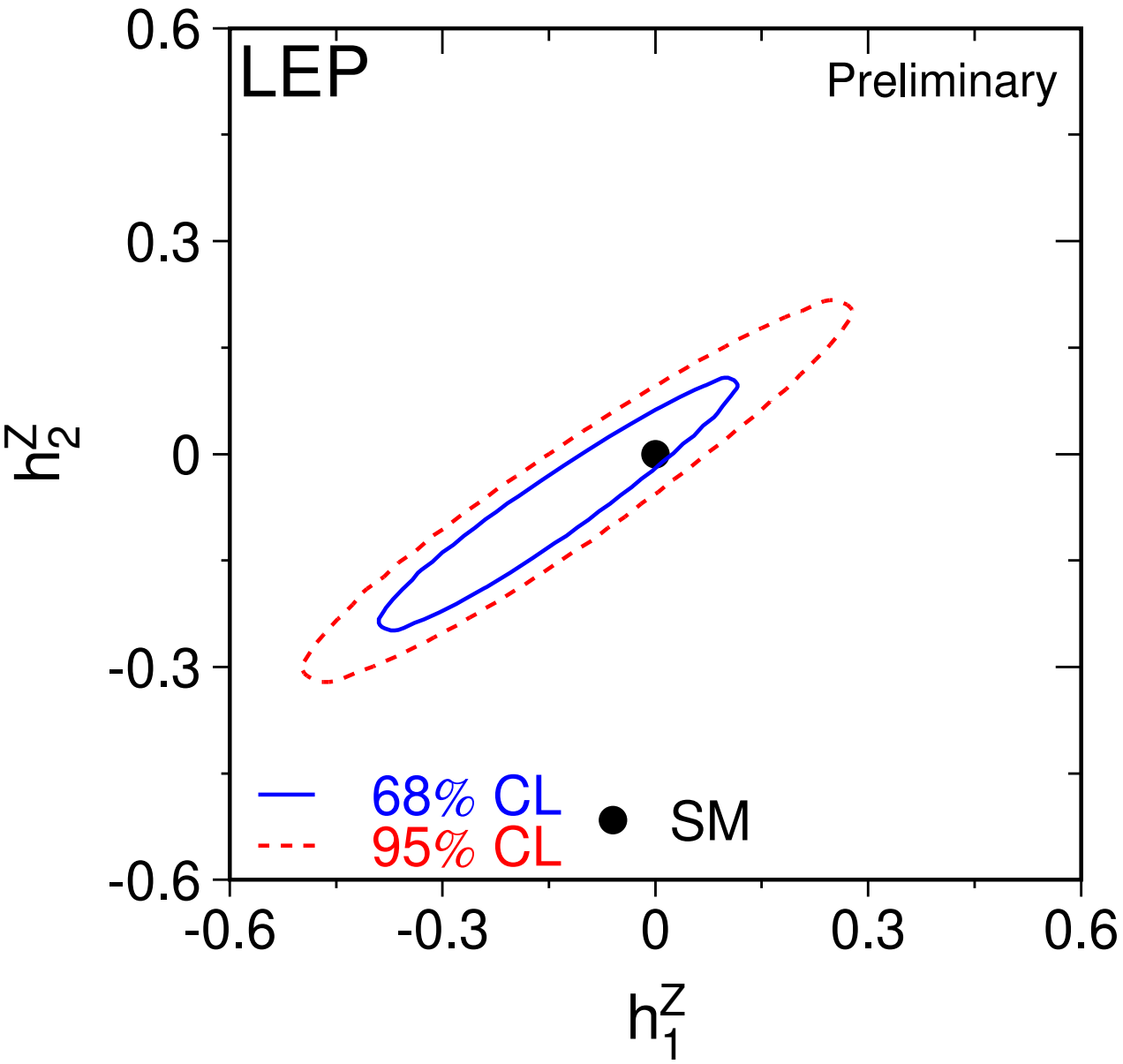

Figure 9: Contour curves of 68% C.L. and 95% C.L. in the plane (h_1^Z, h_2^Z) showing the LEP combined result.

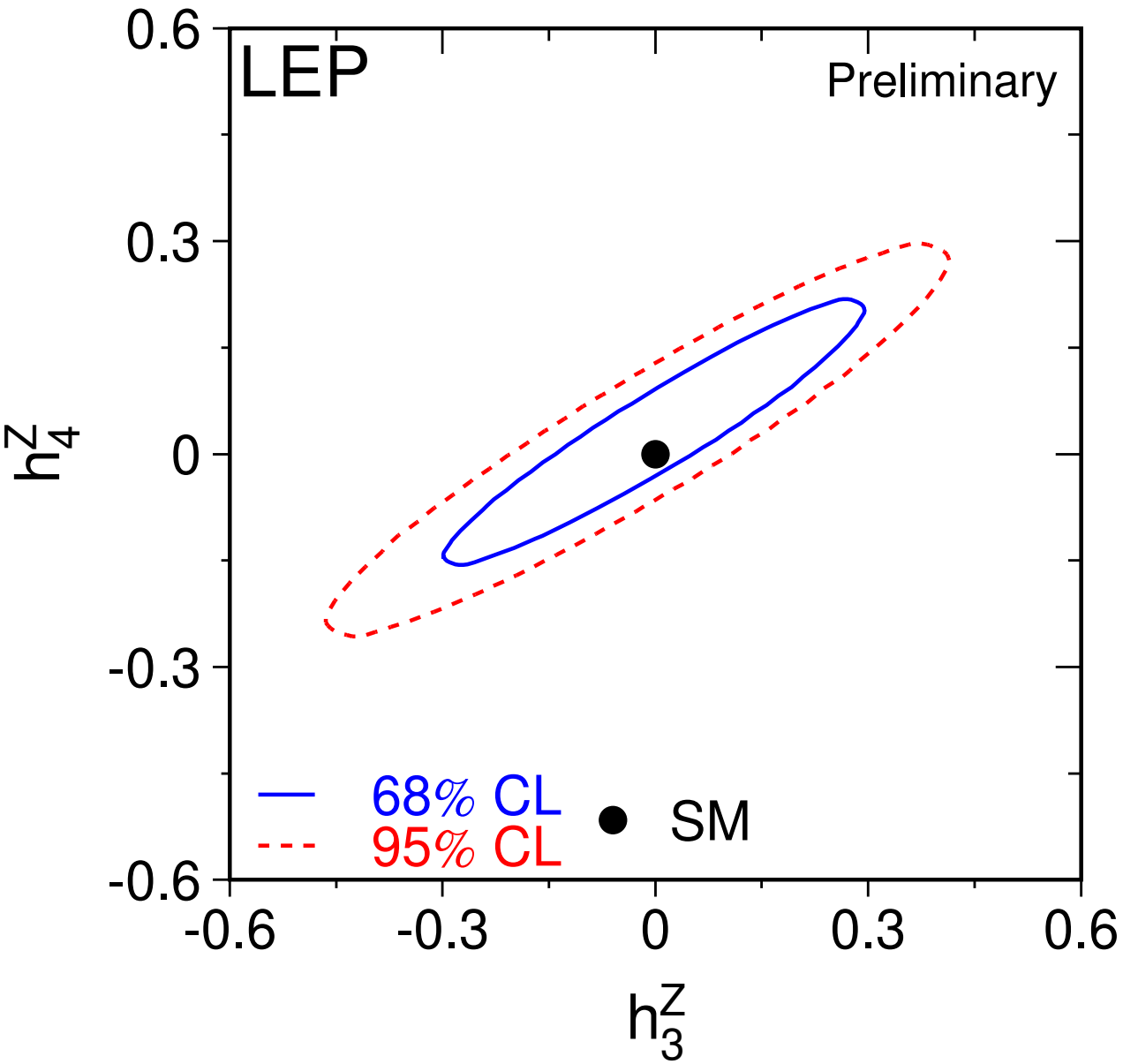

Figure 10: Contour curves of 68% C.L. and 95% C.L. in the plane (h_3^Z, h_4^Z) showing the LEP combined result.

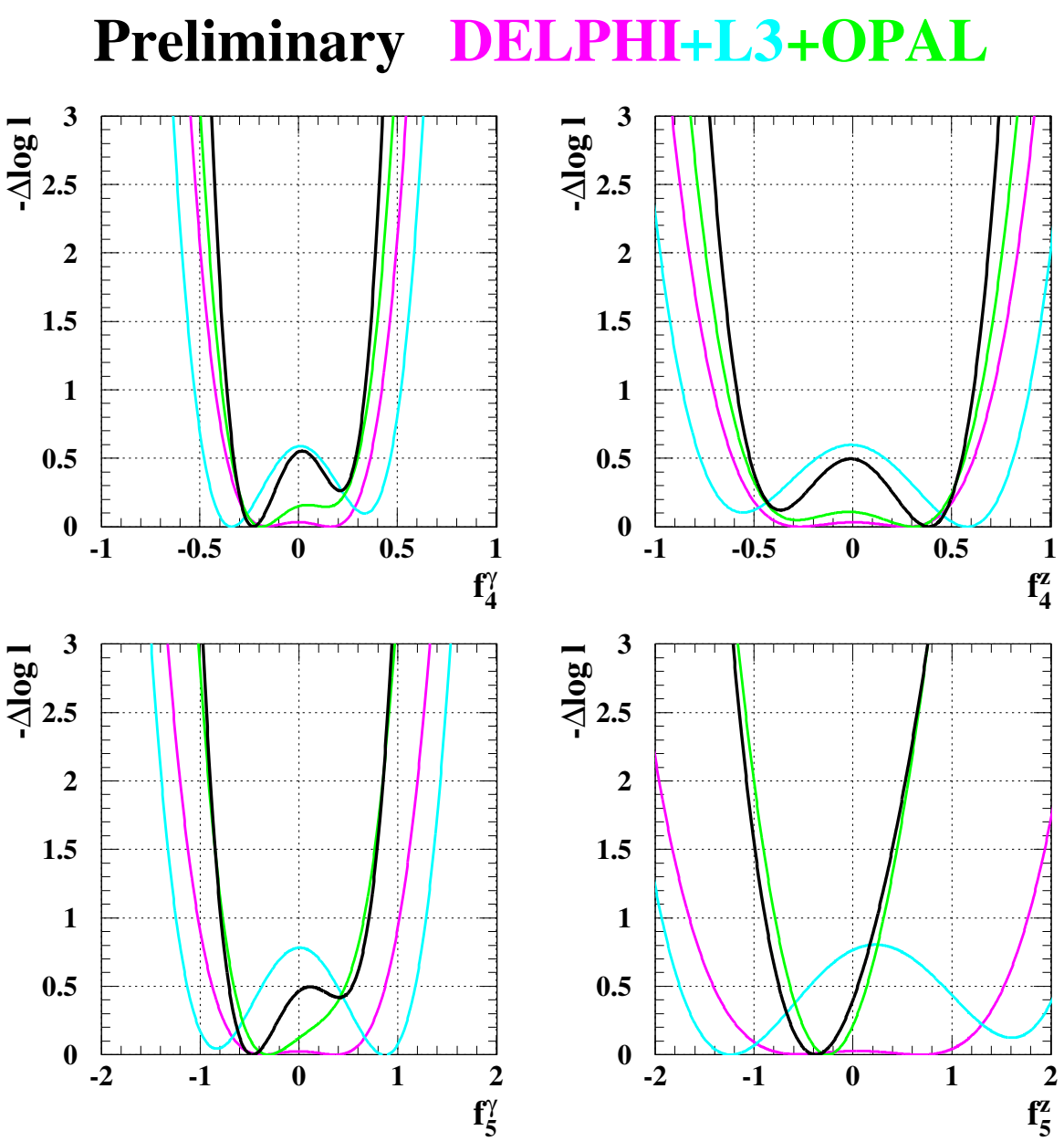

Figure 11: The $\log \mathcal{L}$ curves of DELPHI, L3 and OPAL, and the LEP combined curve for the four neutral TGCs f_i^V, $V = \gamma, Z$, $i = 4, 5$. In each case, the minimal value is subtracted.

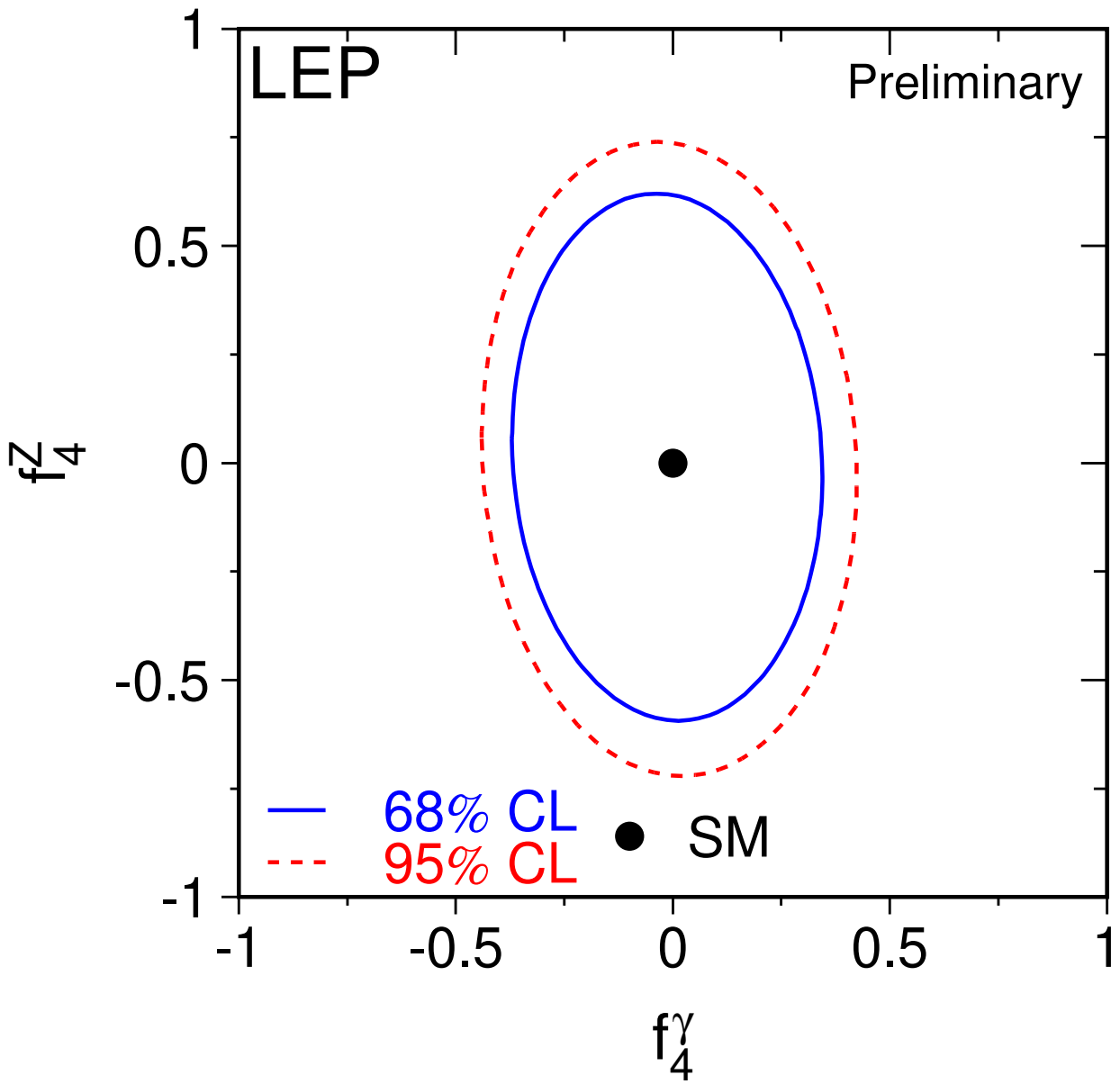

Figure 12: Contour curves of 68% C.L. and 95% C.L. in the plane (f_4^γ, f_4^Z) showing the LEP combined result.

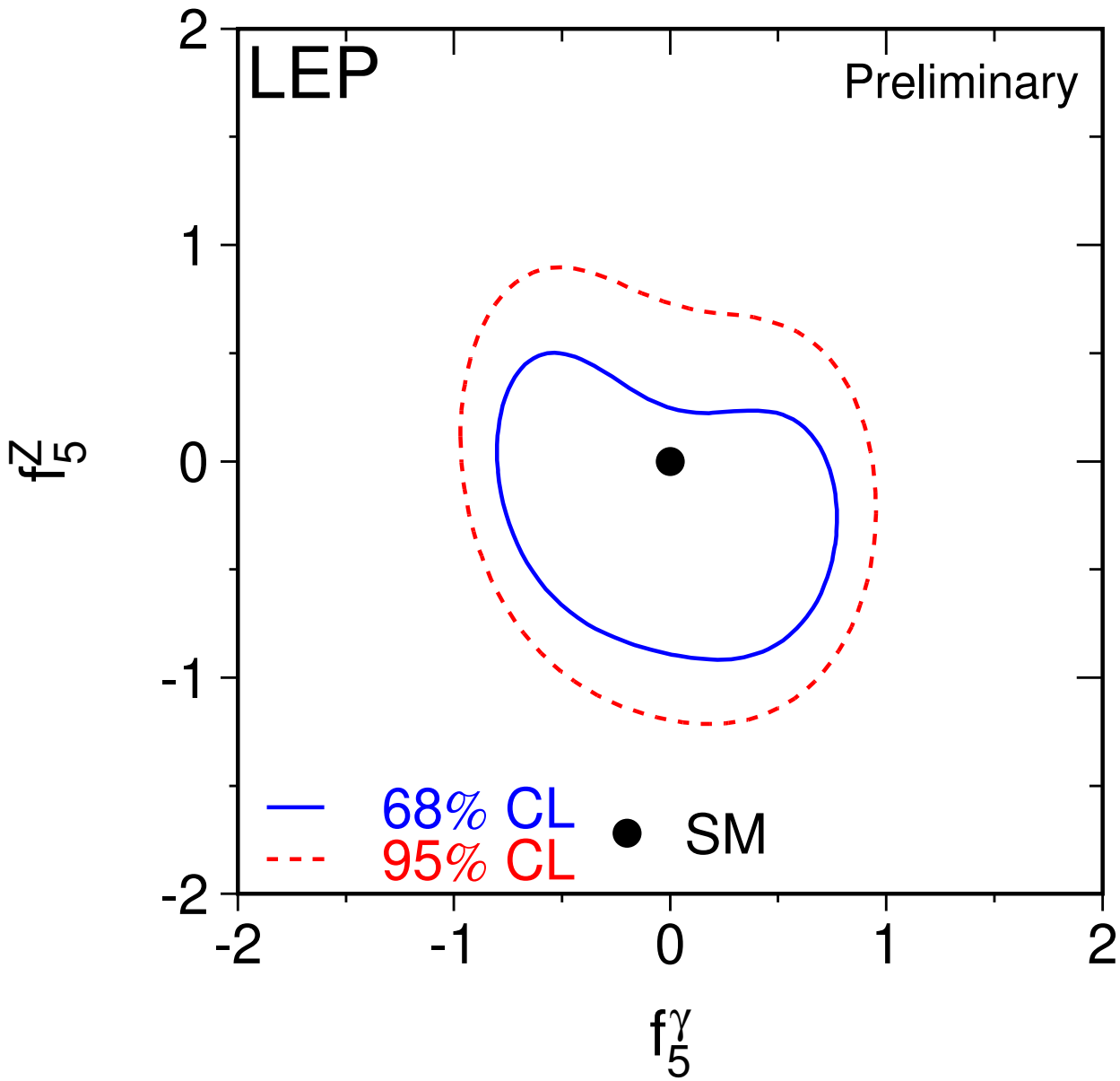

Figure 13: Contour curves of 68% C.L. and 95% C.L. in the plane (f_5^γ, f_5^Z) showing the LEP combined result.

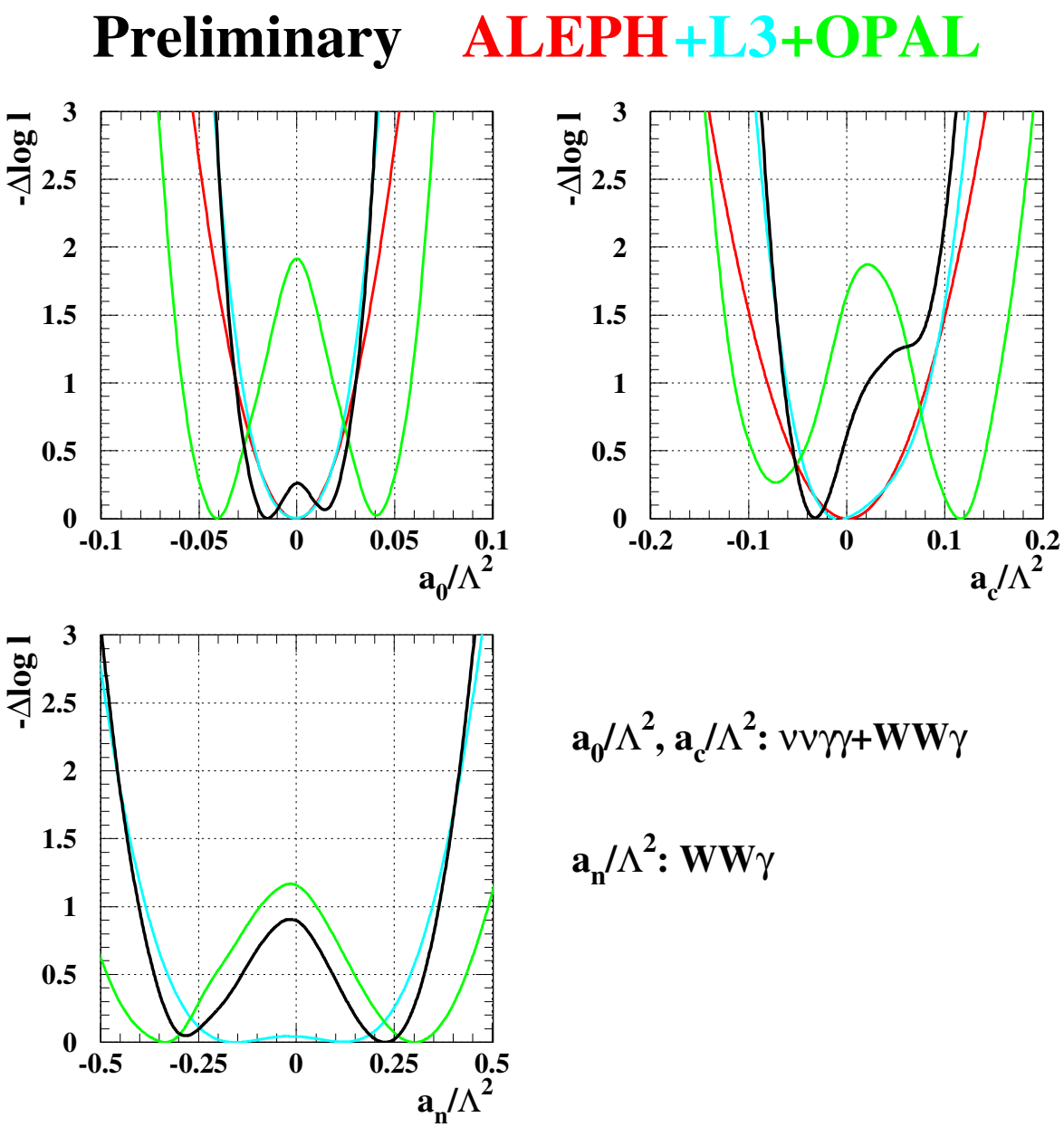

Figure 14: The $\log \mathcal{L}$ curves of ALEPH, L3 and OPAL, and the LEP combined curve for the QGCs derived from WWγ and $\nu\bar{\nu}\gamma\gamma$ production. In each case, the minimal value is subtracted.

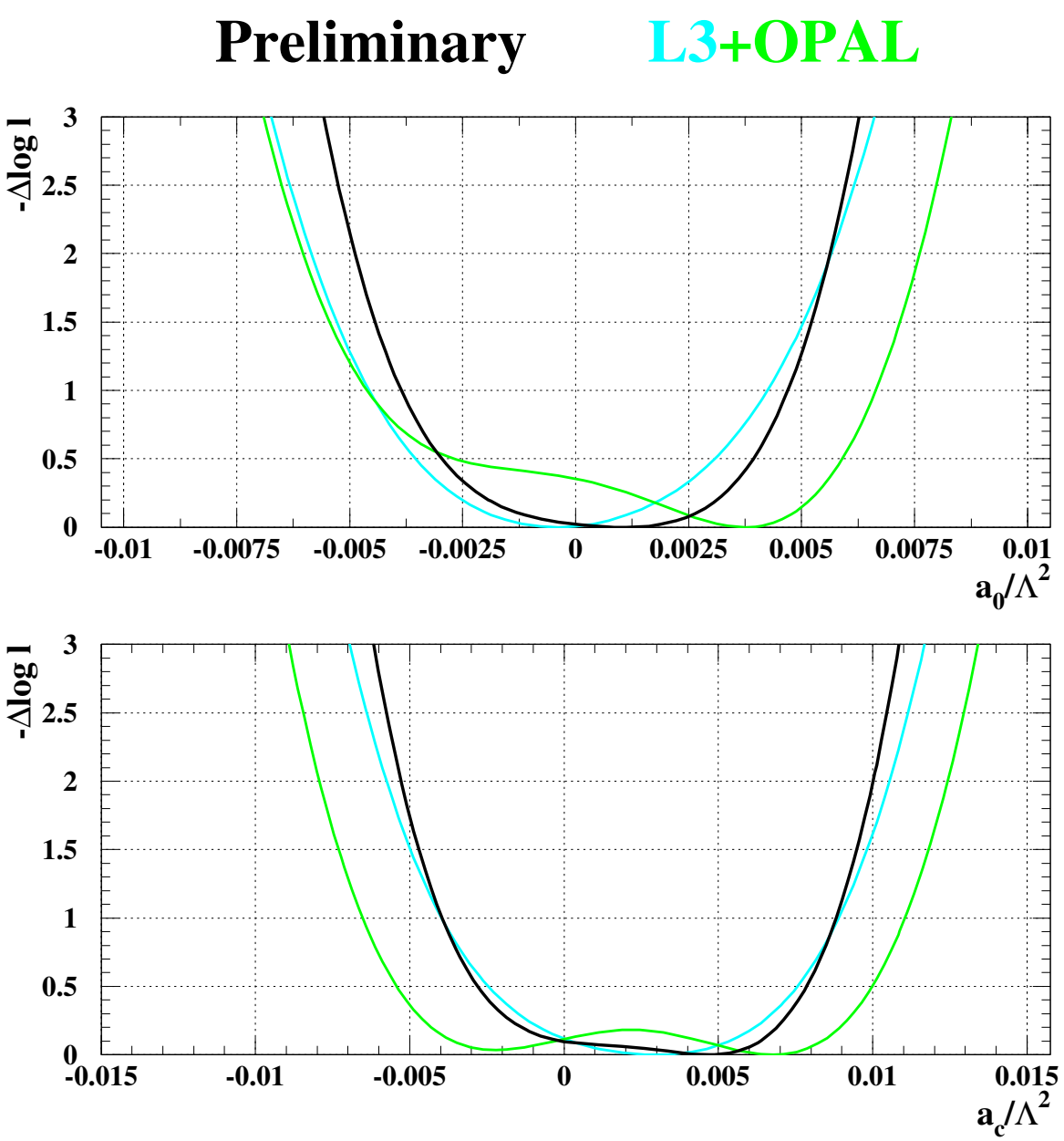

Figure 15: The $\log \mathcal{L}$ curves of L3 and OPAL, and the LEP combined curve for the QGCs derived from $Z\gamma\gamma$ production. In each case, the minimal value is subtracted.